GEOPHYSICS, VOL. 67, NO. 2 (MARCH-APRIL 2002); P. 657–663, 5 FIGS.
10.1190/1.1468627

A stable and efficient approach of inverse *Q* filtering

Yanghua Wang*

ABSTRACT

Stability and efficiency are two issues of general concern in inverse *Q* filtering. This paper presents a stable, efficient approach to inverse *Q* filtering, based on the theory of wavefield downward continuation. It is implemented in a layered manner, assuming a depth-dependent, layered-earth *Q* model. For each individual constant *Q* layer, the seismic wavefield recorded at the surface is first extrapolated down to the top of the current layer and a constant *Q* inverse filter is then applied to the current layer. When extrapolating within the overburden, instead of applying wavefield downward continuation directly, a reversed, upward continuation system is solved to obtain a stabilized solution. Within the current constant *Q* layer, the amplitude compensation operator, which is a 2-D function of traveltime and frequency, is approximated optimally as the product of two 1-D functions depending, respectively, on time and frequency. The constant *Q* inverse filter that compensates simultaneously for phase and amplitude effects is then implemented efficiently in the Fourier domain.

INTRODUCTION

Two fundamental properties associated with wave propagation through subsurface materials are energy dissipation of plane waves with high frequency and velocity dispersion, by which high-frequency plane waves travel faster than low-frequency waves. These effects may be represented mathematically as the earth *Q* filter, defined in terms of a specified *Q* model of the earth (e.g., Futterman, 1962; Strick, 1967, 1970). In seismic data processing where the earth *Q* model is often assumed to be frequency independent (e.g., Kjartansson, 1979), inverse *Q* filtering attempts to compensate recorded seismic signals for these wave propagation effects. Inverse *Q* filtering is a reverse processing of forward wave propagation (Robinson, 1979) and thus may be accomplished by a method similar to seismic deconvolution (Bickel and Natarajan, 1985) or migration (Hargreaves and Calvert, 1991).

Stability and efficiency are two general concerns in any scheme for inverse *Q* filtering. Considering computational efficiency, Hargreaves and Calvert (1991) propose an algorithm akin to Stolt frequency-wavenumber migration (Stolt, 1978). This algorithm, valid for a constant *Q* medium, can efficiently correct for the phase distortion from dispersion but neglects amplitude effect. The amplitude compensation operator is an exponential function of the frequency, and including it in the inverse *Q* filter may cause instability and generate undesirable artifacts in the solution. Therefore, an efficient inverse *Q* filter algorithm that can compensate simultaneously for both phase and amplitude effects without instability is desirable.

I describe the development of such an algorithm based on the theory of wavefield downward continuation. The earth *Q* model is assumed to be a multilayered structure, and inverse *Q* filtering is implemented in a layered manner. For each individual constant *Q* layer, inverse *Q* filtering is accomplished in two steps: (1) the surface-recorded wavefield is extrapolated to the top of the current layer and (2) a constant *Q* inverse filter is performed across that layer. In the first step, the extrapolated wavefield at the top of the current layer may be estimated by solving an inversion system to the downward continuation within the overburden. The solution is stabilized by incorporating a stabilization factor. In the second step, the amplitude operator of the inverse *Q* filter, which is a 2-D function of traveltime and frequency, is approximated optimally as the product of two 1-D functions depending, respectively, on time and frequency. The inverse *Q* filter within the constant *Q* layer is then implemented efficiently by resampling and rescaling in the Fourier domain.

THE INVERSE *Q* FILTER AND NUMERICAL INSTABILITY

Basics of the inverse *Q* filter

The basics of inverse *Q* filtering are summarized to explain the new development in this paper. Inverse *Q* filtering can be based on the 1-D (two-way propagation) wave equation

Manuscript received by the Editor May 15, 2000; revised manuscript received June 25, 2001.
*Robertson Research International Ltd., Horizon House, Azalea Drive, Swanley, Kent BR8 8JR, U.K. E-mail: yanghua@geo.robresint.co.uk.

$$\frac{\partial^2 U(r,\omega)}{\partial r^2} + k^2 U(r,\omega) = 0, \tag{1}$$

where $U(r, \omega)$ is the plane wave of radial frequency ω at travel distance r and k is the wavenumber. Equation (1) has an analytic solution for one-way propagation, given by

$$U(r + \Delta r, \omega) = U(r, \omega) \exp(jk\Delta r), \tag{2}$$

where j is the imaginary unit. Reflection seismograms record the reflection wave along the propagation path r from the source to the reflector and back to the surface. The distance increment Δr can be replaced by

$$\Delta r = v(\omega_0)\Delta T, \tag{3}$$

where $v(\omega_0)$ is the phase velocity at the dominant frequency ω_0 and ΔT is the traveltime increment. The earth Q effect is introduced in the definition of the wavenumber k:

$$k = \frac{\omega}{v(\omega)}\left(1 - \frac{j}{2Q}\right), \tag{4}$$

where $v(\omega)$ is the frequency-dependent phase velocity and Q is the medium quality factor, which is assumed to be frequency independent. Substituting the complex-valued wavenumber k into solution (2), we have the expression of inverse Q filter,

$$U(T + \Delta T, \omega) = U(T, \omega) \exp\left(\frac{j\omega v(\omega_0)}{v(\omega)}\Delta T\right) \times \exp\left(\frac{\omega v(\omega_0)}{2Qv(\omega)}\Delta T\right). \tag{5}$$

The two exponential operators compensate for, respectively, the phase effect (i.e., velocity dispersion) and the amplitude effect (i.e., energy absorption) of the earth Q filter.

In the following computation, I use a model for the phase velocity $v(\omega)$ defined by

$$v(\omega) = v(\omega_0)\left|\frac{\omega}{\omega_0}\right|^{\gamma}, \tag{6}$$

where

$$\gamma = \frac{2}{\pi}\tan^{-1}\left(\frac{1}{2Q}\right) \approx \frac{1}{\pi Q} \tag{7}$$

(Kjartansson, 1979). Inverse Q filter (5) is then rewritten as

$$U(T + \Delta T, \omega) = U(T, \omega) \exp\left(j\left|\frac{\omega}{\omega_0}\right|^{-\gamma}\omega\Delta T\right) \times \exp\left(\left|\frac{\omega}{\omega_0}\right|^{-\gamma}\frac{\omega\Delta T}{2Q}\right). \tag{8}$$

Equation (8) is the basis for an inverse Q filter in which downward continuation is performed on all plane waves in the frequency domain. The sum of these plane waves then gives the time-domain seismic signal,

$$u(T + \Delta T) = \frac{1}{2\pi}\int U(T + \Delta T, \omega)\, d\omega. \tag{9}$$

Equations (8) and (9) must be applied successively to each time sample with sampling interval ΔT, producing $u(T)$ at each level.

Numerical instability

The basic downward continuation scheme described above is now tested on noise-free synthetic seismic traces, which clearly show the numerical instability of the inverse Q filter.

A synthetic trace is built by

$$u(t) = \Re\left\{\frac{1}{\pi}\int_0^{\infty} S(\omega)\exp[j(\omega t - kr)]\, d\omega\right\}, \tag{10}$$

where $S(\omega)$ is the Fourier transform of a source waveform $s(t)$ defined as the real-valued Ricker wavelet,

$$s(t) = \left(1 - \frac{1}{2}\omega_0^2 t^2\right)\exp\left(-\frac{1}{4}\omega_0^2 t^2\right), \tag{11}$$

with the dominant radial frequency $\omega_0 = 100\pi$ (i.e., 50 Hz). The Ricker wavelet is a symmetric, noncausal wavelet. I use this symmetric wavelet to conveniently examine the phase change visually after the inverse Q filter is applied, although a minimum phase wavelet such as the Berlage wavelet (Aldridge, 1990) would be more realistic for the source function.

Given the travel distance $r = v(\omega_0)t_r$ for traveltime t_r of the plane wave with dominant frequency ω_0, equation (4) provides the term kr used in equation (10):

$$kr = \left(1 - \frac{j}{2Q}\right)\left|\frac{\omega}{\omega_0}\right|^{-\gamma}\omega t_r, \tag{12}$$

independent of the velocity $v(\omega_0)$. In the example, I consider the signal to consist of a sequence of Ricker wavelets with $t_r = 100, 400, \ldots, 1900$ ms (increment of 300 ms). Figure 1a

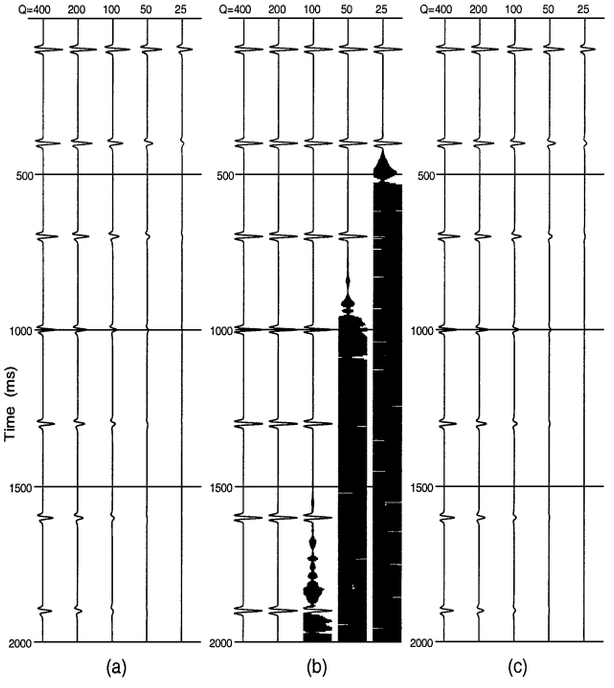

FIG. 1. The earth Q filter and the inverse Q filter. (a) Synthetic traces show the effect of the earth Q filter with $Q = 400$, 200, 100, 50, and 25. (b) The inverse Q filtering (compensating for both phase and amplitude) result, which clearly indicates numerical instability. (c) The phase-only inverse Q filtering result.

shows five synthetic traces with different Q values ($Q = 400$, 200, 100, 50, and 25) constant with depth in each case.

The result of applying the inverse Q filter to the synthetic signals is displayed in Figure 1b. For traces with $Q = 400$ and 200, the process restores the Ricker wavelet with correct phase and amplitude. However, there are strong artifacts as the Q value decreases and the imaging time T increases, even though the input signal is noise free. The appearance of noise in the output signal is a natural consequence of the downward continuation procedure: A plane wave is attenuated gradually, but beyond a certain distance the signal is below the ambient noise level. The amplification required to recover the signal amplifies the ambient noise. In the data-noise-free case here, the background noise is the machine errors relative to working precision. The cause of strong artifacts is referred to as the numerical instability of the inverse Q filter.

The stability condition may be stated as

$$\Lambda(\omega) \equiv \exp\left(\left|\frac{\omega}{\omega_0}\right|^{-\gamma} \frac{\omega \Delta T}{2Q}\right) \le 1, \tag{13}$$

where $\Lambda(\omega)$ is the amplitude compensation operator in equation (8). If we set $\Lambda(\omega) = 1$, the inverse Q filter for phase-only compensation is unconditionally stable, as shown in Figure 1c.

The artifacts caused by numerical instability can be suppressed by a low-pass filter. Based on experiments, I have found the following empirical stability condition:

$$\exp\left(\left|\frac{\omega}{\omega_0}\right|^{-\gamma} \frac{\omega}{2Q} \sum \Delta T\right) \le e, \tag{14}$$

that is, the (accumulated) exponent of the amplitude factor is not greater than 1. Equation (14) thus suggests an upper limit on the frequencies that could be included in the amplitude compensation,

$$\omega \le \frac{2Q}{T} \equiv \omega_q, \tag{15}$$

which has a time-varying frequency limit. I test this low-pass filter in the following three alternative ways:

1. Both phase and amplitude compensation are truncated at frequency ω_q with cosine-squared tapering;
2. Phase compensation is performed on the full frequency band but with amplitude compensation only within the band limit $[0, \omega_q)$;
3. Both phase and amplitude are compensated on the full-frequency band with the amplitude operator defined by

$$\Lambda(\omega) = \begin{cases} \exp\left(\left|\dfrac{\omega}{\omega_0}\right|^{-\gamma} \dfrac{\omega \Delta T}{2Q}\right), & \omega \le \omega_q \\ \Lambda(\omega_q), & \omega > \omega_q \end{cases}. \tag{16}$$

The results of these three schemes applied to the synthetic data set of Figure 1a are shown in Figures 2a, 2b, and 2c, respectively. Figure 2b shows improvement over Figure 2a, but Figure 2c is superior to both because the amplitudes for the traces $Q \le 200$ are better compensated. In each case the numerical instability evident in Figure 1b is successfully suppressed. The third test scheme (Figure 2c) is called a gain-limited inverse Q filter.

THE STABLE, EFFICIENT APPROACH

Layered implementation

In the basic inverse Q filtering scheme above, the extrapolation step ΔT is the sample rate of the digitized seismic trace, while the output at each sample point is required. The computational demands of this samplewise downward continuation render it impractical for routine prestack seismic processing. Since the inverse Q filter works on individual traces, it is reasonable to divide the depth-dependent earth Q model into a series of constant Q layers and to implement the inverse Q filter in a layered manner. This procedure is shown in Figure 3.

The idea behind the layered model algorithm is to treat the top of the current layer as a new recording surface and thereby apply a fast algorithm of inverse Q filter to the constant Q layer. Lowering the recording surface to the level of the top of the current layer is accomplished by the downward continuation of expression (8). This step is very fast since equation (8) is applied in one step for the traveltime across each layer in the overburden.

Suppose we divide the earth Q model into N layers defined by interfaces at two-way traveltimes T_n for $n = 1, \ldots, N-1$, with $T_0 = 0$ and T_N being the maximum record time. The plane-wave downward continuation from the surface to the top of the nth layer can be implemented recursively:

$$U(T_0, \omega) \to U(T_1, \omega) \to \cdots \to U(T_{n-1}, \omega). \tag{17}$$

Each step is given explicitly by

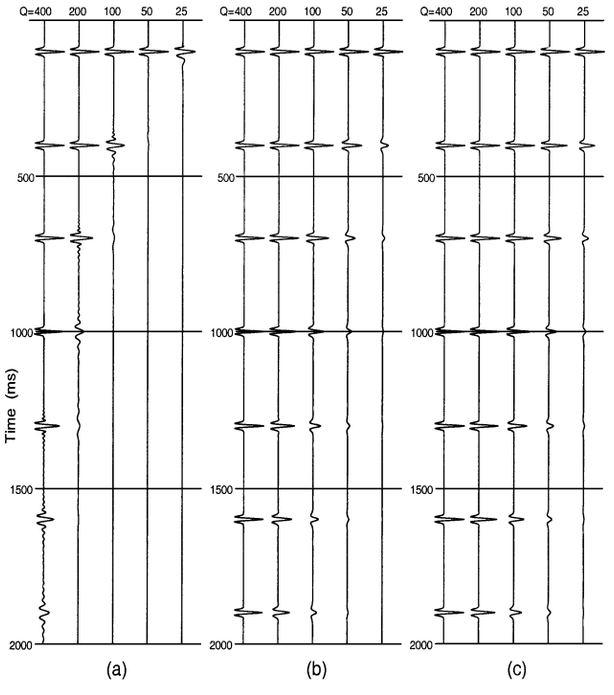

FIG. 2. Inverse Q filter using three distinct methods: (a) with a low-pass filter, $\omega \le \omega_q$; (b) with full-band phase compensation but band-limited amplitude compensation; (c) with full-band phase compensation and modified full-band amplitude compensation, i.e., the gain-limited inverse Q filter. The input signal in each case is as shown in Figure 1a.

$$U(T_{n-1},\omega) = U(T_{n-2},\omega)\exp\left(j\left|\frac{\omega}{\omega_0}\right|^{-\gamma_{n-1}}\omega\Delta T_{n-1}\right) \times \exp\left(\left|\frac{\omega}{\omega_0}\right|^{-\gamma_{n-1}}\frac{\omega\Delta T_{n-1}}{2Q_{n-1}}\right), \quad (18)$$

where $\Delta T_{n-1} = T_{n-1} - T_{n-2}$ is the thickness of the $(n-1)$th layer, in which Q_{n-1} is constant, and $\gamma_{n-1} = 1/(\pi Q_{n-1})$. Downward continuation using equation (18), performed on all frequencies, compensates accurately for the effect of earth Q filter between the surface and the top of the current layer.

The extrapolated wavefield $U(T_{n-1},\omega)$ is then used as the input of the inverse Q filter within the nth layer. For clarity, I refer to T_{n-1} as the origin of a reduced time coordinate τ and denote the wavefield recorded at level T_{n-1} as

$$M(\tau = 0,\omega) \equiv U(T_{n-1},\omega). \quad (19)$$

Blending expressions (8) and (9) into one form, the inverse Q-filtered seismic trace may be presented in the time-shifted domain:

$$m(\tau) = \frac{1}{2\pi}\int M(0,\omega)\exp\left(j\left|\frac{\omega}{\omega_0}\right|^{-\gamma}\omega\tau\right) \times \exp\left(\left|\frac{\omega}{\omega_0}\right|^{-\gamma}\frac{\omega\tau}{2Q}\right)d\omega, \quad (20)$$

where the layer subscript to parameter Q is dropped. As depicted in Figure 3, only the front portion of $m(\tau)$ is stored into output $u(T)$,

$$u(T_{n-1}+\tau) = m(\tau), \quad (21)$$

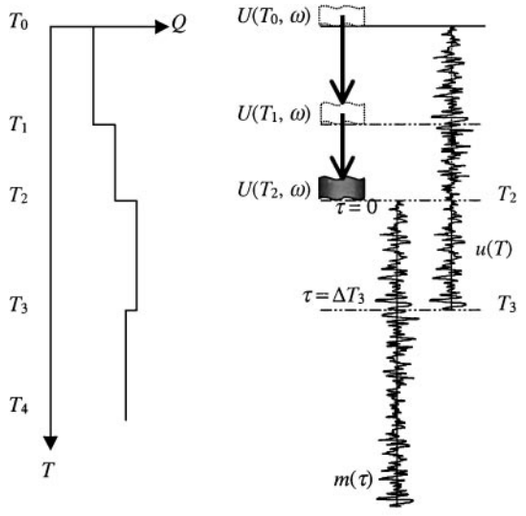

FIG. 3. Earth Q model divided into N layers with the base of layer n at two-way times T_n. The inverse Q filtering is implemented in a layered manner. The double wave symbol represents the plane wave U; the vertical arrow indicates the downward continuation. The result of inverse Q filtering within a constant Q layer is the portion of $m(\tau)$ for $\tau \in [0,\ \Delta T_n]$, which is stored to the output trace $u(T)$ for $T \in [T_{n-1}, T_n]$.

where $\tau \in [0, \Delta T_n]$ and $\Delta T_n = T_n - T_{n-1}$ is the thickness of the nth layer.

Stabilized downward continuation

In the downward continuation step across the overburden [equation (18)], the gain-limited inverse Q filtering scheme with the amplitude operator given by expression (16) could be applied. However, to further improve the performance, I propose a stabilized approach to the wavefield extrapolation within the overburden.

Instead of directly applying the downward continuation, I establish a reversed system and solve it to obtain the extrapolated wavefield. Suppose the wavefield $U(T_{n-1},\omega)$ at the top of the nth layer is obtained from the recursive downward continuation using equation (17). That is,

$$U(T_{n-1},\omega) = \alpha(\omega)U(T_0,\omega), \quad (22)$$

where $\alpha(\omega)$ is the extrapolation operator. The reversed, upward continuation system

$$U(T_{n-1},\omega) \to \cdots \to U(T_1,\omega) \to U(T_0,\omega) \quad (23)$$

is represented by

$$U(T_0,\omega) = \beta(\omega)U(T_{n-1},\omega), \quad (24)$$

where $\beta(\omega)$ is the operator of the upward continuation system. Wavefield $U(T_{n-1},\omega)$ is then estimated by

$$U(T_{n-1},\omega) = \frac{\beta^*(\omega)}{\beta^*(\omega)\beta(\omega)+\sigma^2}U(T_0,\omega), \quad (25)$$

where β^* is the conjugate of β and σ^2 is a real positive constant used to stabilize the solution.

The operator $\beta(\omega)$ of the reversed upward continuation system, which is in fact the forward earth Q filter, may be given explicitly as

$$\beta(\omega) = \exp\left[-\sum_{\ell=1}^{n-1}\left(\frac{1}{2Q_\ell}+j\right)\left|\frac{\omega}{\omega_0}\right|^{-\gamma_\ell}\omega\Delta T_\ell\right]. \quad (26)$$

The sum in the exponent is also calculated recursively.

Inverse Q filtering within a constant Q layer

I now describe how to implement inverse Q filtering within a constant Q layer. To obtain computational efficiency, three different approximations to the amplitude operator are tested.

Using a new variable

$$\omega' = \omega\left|\frac{\omega}{\omega_0}\right|^{-\gamma}, \quad (27)$$

equation (20) is rewritten as

$$m(\tau) = \frac{1}{2\pi}\int M(0,\omega')J\Lambda(\tau,\omega')\exp(j\omega'\tau)\,d\omega', \quad (28)$$

where $M(0,\omega') \equiv M(0,\omega(\omega'))$ is resampled from $M(0,\omega)$ to $M(0,\omega')$, J is the Jacobian

$$J \equiv \left\|\frac{d\omega}{d\omega'}\right\| = \frac{1}{1-\gamma}\left|\frac{\omega'}{\omega_0}\right|^{\gamma/(1-\gamma)}, \quad (29)$$

and Λ is the amplitude compensation operator

$$\Lambda(\tau, \omega') = \exp\left(\frac{\omega'\tau}{2Q}\right). \quad (30)$$

The amplitude compensation operator is omitted by Hargreaves and Calvert (1991), and their phase-only compensation algorithm is implemented using interpolation and scaling in the Fourier domain. Their method is fast because it is based on the fast Fourier transform. I retain the amplitude operator $\Lambda(\tau, \omega')$ in equation (28) but use an approximation to it so the fast Fourier transform can still be used.

Given a layer with moderate thickness indicated by two-way traveltime ΔT, one can approximate $\Lambda(\tau, \omega')$ by averaging over this time window:

$$\begin{aligned}\Lambda_1(\omega') &= \frac{1}{\Delta T}\int_0^{\Delta T} \exp\left(\frac{\omega'\tau}{2Q}\right) d\tau \\ &\approx 1 + \frac{\omega'\Delta T}{4Q} + \frac{1}{6}\left(\frac{\omega'\Delta T}{2Q}\right)^2. \end{aligned} \quad (31)$$

Expression (28) is then written as

$$m(\tau) = \frac{1}{2\pi}\int M(0, \omega') J \Lambda_1(\omega') \exp(j\omega'\tau)\, d\omega'. \quad (32)$$

The evaluation of equation (32) thus involves the following steps: interpolating $M(0, \omega)$ to $M(0, \omega')$ with evenly spaced values of ω', scaling with the Jacobian J, amplitude compensation $\Lambda_1(\omega')$, and finally the inverse Fourier transform. If one sets $\Lambda_1(\omega') = 1$, expression (32) represents the phase-only inverse filter. Thus, the amplitude operator $\Lambda_1(\omega')$ acts as a band-pass filter applied to the phase-corrected seismic trace. The bandwidth is the useful frequency range of the seismic signal. Although there is no need for a low cutoff frequency definition, tapering is required at the high cutoff frequency edge.

Instead of averaging over the time window, one can alternatively replace the 2-D amplitude operator in equation (28) by its average over the frequency band:

$$\begin{aligned}\Lambda_2(\tau) &= \frac{1}{\Delta\omega'}\int_{\omega'_c-\Delta\omega'/2}^{\omega'_c+\Delta\omega'/2} \exp\left(\frac{\omega'\tau}{2Q}\right) d\omega' \\ &\approx \left[1 + \frac{1}{6}\left(\frac{\Delta\omega'\tau}{4Q}\right)^2\right]\exp\left(\frac{\omega'_c\tau}{2Q}\right), \end{aligned} \quad (33)$$

where ω'_c is the center frequency of the frequency band and $\Delta\omega'$ is the bandwidth. Both ω'_c and $\Delta\omega'$ may vary with time. Expression (28) then becomes

$$m(\tau) = \Lambda_2(\tau)\left[\frac{1}{2\pi}\int M(0, \omega') J \exp(j\omega'\tau)\, d\omega'\right], \quad (34)$$

where the band-limited gain $\Lambda_2(\tau)$ is applied to the phase-only corrected seismic trace. This gain compensation can be used in conjunction with the compensation of the offset-dependent spherical divergence to remove the need for any trace equalization or automatic gain control prior to, for example, an energy-preserving deconvolution.

The function Λ_1 is a 1-D function of the frequency, whereas Λ_2 depends on the traveltime. In a third method, I approximate the 2-D amplitude operator as a product of two 1-D functions

$$\Lambda_3(\tau, \omega') = \Lambda_{31}(\tau)\Lambda_{32}(\omega'). \quad (35)$$

Splitting the exact amplitude operator (30) into

$$\Lambda(\tau, \omega') = \exp\left(\frac{\omega'_c}{2Q}\tau\right)\exp\left(\frac{\omega' - \omega'_c}{2Q}\tau\right), \quad (36)$$

I define the time-dependent term at the central frequency ω_c,

$$\Lambda_{31}(\tau) = \exp\left(\frac{\omega'_c}{2Q}\tau\right), \quad (37)$$

and the frequency-dependent term based on the average over the time interval ΔT,

$$\begin{aligned}\Lambda_{32}(\omega') &= \frac{1}{\Delta T}\int_0^{\Delta T} \exp\left(\frac{\omega' - \omega'_c}{2Q}\tau\right) d\tau \\ &\approx 1 + \frac{\Delta T}{4Q}(\omega' - \omega'_c) + \frac{\Delta T^2}{24Q^2}(\omega' - \omega'_c)^2. \end{aligned} \quad (38)$$

The inverse Q filter [equation (28)] is then

$$\begin{aligned} m(\tau) = \Lambda_{31}(\tau)\Bigg[\frac{1}{2\pi}\int M(0, \omega') J \Lambda_{32}(\omega') \\ \times \exp(j\omega'\tau)\, d\omega'\Bigg], \end{aligned} \quad (39)$$

where the time gain function Λ_{31} is applied following the inverse Fourier transform.

Figure 4 compares numeric errors of the three approximations (Λ_1, Λ_2, and Λ_3) against the exact amplitude operator Λ. The radius of the circles indicates the magnitude of the errors. These errors are estimated based on an example model of $Q = 50$ within the 300-ms time window and the 10- to 90-Hz frequency band. Errors (ε values) on the upper boundaries are given explicitly in the figure. The best alternative among these three is $\Lambda_3 = \Lambda_{31}\Lambda_{32}$, which is used in the following examples.

Summary

The stabilized layered inverse Q filtering method uses equation (25) to extrapolate the surface-recorded wavefield to the top of the current layer, and then equation (39) within the current constant Q layer, to produce the Q compensated output across the layer. The procedure is repeated for all constant Q layers.

This layered implementation is akin to recursive migration, a name that emphasizes the recursive calculation of the downward continuation (Kim et al., 1989). I refer to this procedure as the layered method because the result of a specific layer is independent of the output within the overburden. This property also contrasts with a layer-stripping implementation.

APPLICATION AND DISCUSSION

Example results

To demonstrate the effectiveness of this algorithm, Figure 5 displays three sets of results for the layered inverse Q filter: (a) phase compensation only; (b) compensation for both phase and amplitude, but the downward continuation within the overburden using the gain-limited inverse Q filter with the amplitude operator defined in expression (16); and (c) the stabilized solution based on equations (25) and (39) with $\sigma^2 = 10^{-4}$.

Figures 5a and 5b, the results for phase only and for both phase and amplitude, are similar to Figures 1c and 2c,

respectively. The accuracy of this layered scheme is very close to that of the basic sample scheme. But the layered method is much faster than the latter. For this particular example, the sample rate of the synthetic traces is 2 ms, whereas the thickness used in the layered scheme is 300 ms. That is, seven layers are involved in the computation.

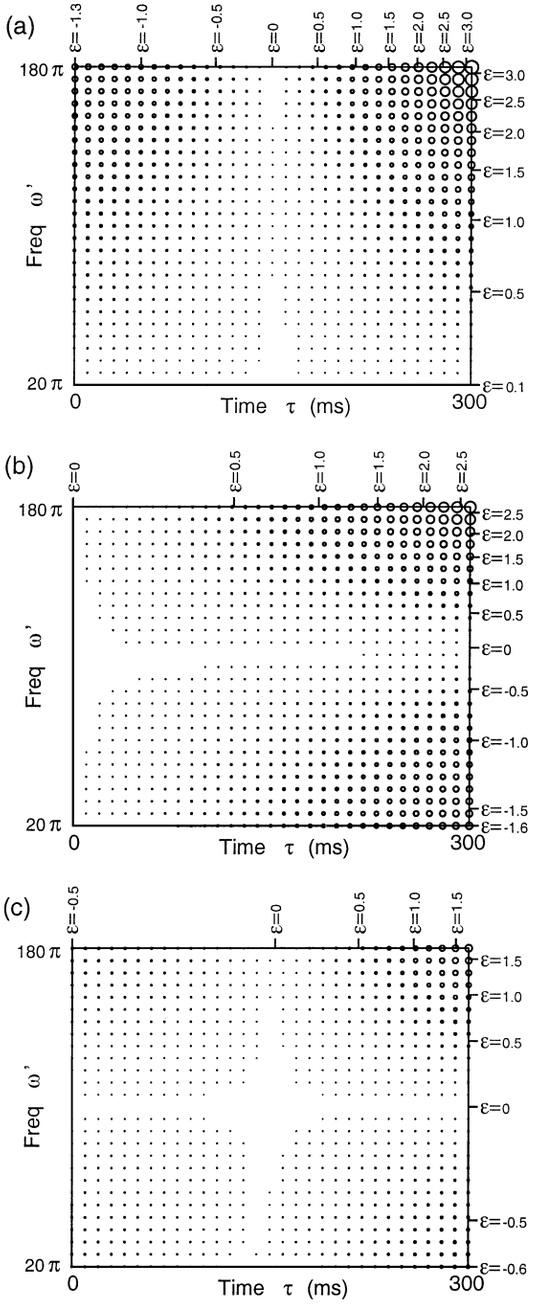

FIG. 4. Numerical errors of the three approximations Λ_1 [equation (31)], Λ_2 [equation (33)], and Λ_3 [equation (35)], relative to the exact amplitude operator Λ [equation (30)]: (a) $\Lambda - \Lambda_1$, (b) $\Lambda - \Lambda_2$, and (c) $\Lambda - \Lambda_3$. These errors are estimated based on an example model of $Q = 50$ within the 300-ms time window and the 10–90-Hz frequency band. The radius of each circle is proportional to the absolute value of the error, where specific error values (ε) are indicated on the upper boundaries.

From Figure 5c, we see clearly that the amplitudes of more high-frequency components are compensated by using the stabilized computation scheme. We have recovered all components that in principle are recoverable, if we compare Figures 5c and 1b. The stabilized solution intelligently limits the attempt to compensate the highly attenuated high-frequency plane waves propagating through a low Q medium.

Discussion

When the inverse Q filter is applied to real seismic data, high-frequency noise is also amplified since the amplitude compensation operator is an exponential function of the frequency. To overcome this problem, I use spatial linear prediction theory, prior to the inverse Q filtering, to extract coherent signal from the seismic data (Wang, 1999). Noise traces, given by the difference between the original traces and predicted traces, could be mixed back to the resultant traces after the inverse Q filtering on predicted noise-free traces.

For a seismic gather, inverse Q filtering working on each single trace takes the offset effect into account. Suppose the multilayered Q model is a 1-D function defined at zero offset, $Q(T, 0)$. The Q function for a nonzero offset trace is approximated by

$$Q(T, x) = Q\left(\sqrt{T^2 - \frac{x^2}{v_{\text{nmo}}^2}}, 0\right), \tag{40}$$

where x is the source–receiver offset and v_{nmo} is the NMO velocity.

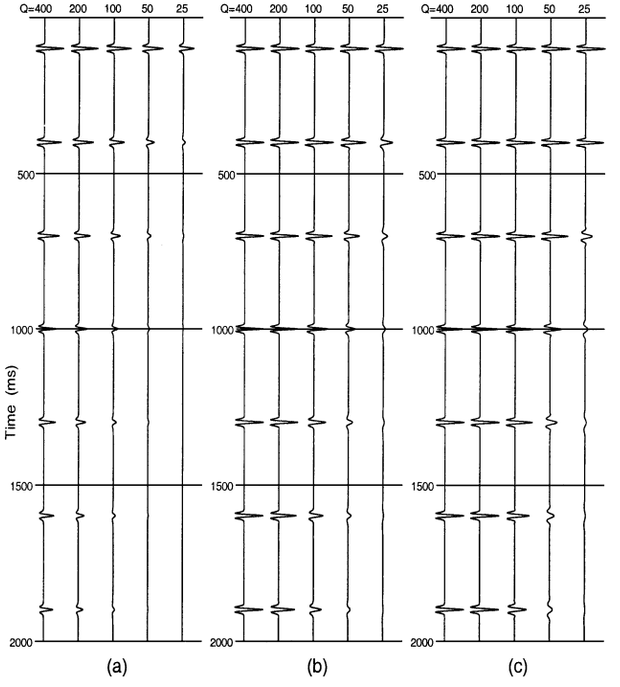

FIG. 5. Layered inverse Q filtering: (a) compensating for phase only; (b) compensating for both phase and amplitude, where the extrapolation through the overburden uses the gain-limited inverse Q filter scheme; (c) compensating for both phase and amplitude, where wavefield extrapolation uses the stabilized algorithm, which recovers all components that in principle are recoverable.

Inverse *Q* filtering for marine seismic data normally should start from the water bottom. The downward continuation method presented here, starting from the surface, includes the water layer, in which $1/Q = 0$. The effective *Q* function below the water is generally assumed to be proportional to the layer velocity. It would be better to overestimate *Q* than to underestimate *Q*, according to the sensitivity analysis by Duren and Trantham (1997).

CONCLUSION

A stable, efficient approach to inverse *Q* filtering is presented for a multilayered-earth *Q* model. For each constant *Q* layer, the stabilized solution to the wavefield downward continuation within the overburden combined with the optimal approximation to the compensation operator within the current layer characterize this elegant algorithm for the inverse *Q* filter.

ACKNOWLEDGMENTS

Thanks to Stuart Merrylees for drawing my attention to this subject and to Greg Houseman for a critical reading of the manuscript. The paper is published with permission from Robertson Research International Ltd.

REFERENCES

Aldridge, D. F., 1990, The Berlage wavelet: Geophysics, **55**, 1508–1511.
Bickel, S. H., and Natarajan, R. R., 1985, Plane-wave *Q* deconvolution: Geophysics, **50**, 1426–1439.
Duren, R. E., and Trantham, E. C., 1997, Sensitivity of the dispersion correction to *Q* error: Geophysics, **62**, 288–290.
Futterman, W. I., 1962, Dispersive body waves: J. Geophys. Res., **67**, 5279–5291.
Hargreaves, N. D., and Calvert, A. J., 1991, Inverse *Q* filtering by Fourier transform: Geophysics, **56**, 519–527.
Kim, Y. C., Gonzalez, R., and Berryhill, J. R., 1989, Recursive wavenumber-frequency migration: Geophysics, **54**, 319–329.
Kjartansson, E., 1979, Constant *Q* wave propagation and attenuation: J. Geophys. Res., **84**, 4737–4748.
Robinson, J. C., 1979, A technique for the continuous representation of dispersion in seismic data: Geophysics, **44,** 1345–1351.
Stolt, R. H., 1978, Migration by Fourier transform: Geophysics, **43**, 23–48.
Strick, E., 1967, The determination of *Q*, dynamic viscosity and transient creep curves from wave propagation measurements: Geophys. J. Roy. Astr. Soc., **13**, 197–218.
——— 1970, A predicted pedestal effect for pulse propagation in constant-*Q* solids: Geophysics, **35**, 387–403.
Wang, Y., 1999, Random noise attenuation using forward-backward linear prediction: J. Seis. Expl., **8**, 133–142.